Published in final edited form as:
Biochemistry. 2009 November 3; 48(43): 10286–10297. doi:10.1021/bi9013775.

GPR37 Surface Expression Enhancement via N-Terminal Truncation or Protein-Protein Interactions[1]

Jill H. Dunham, **Rebecca C. Meyer**, **Erin L. Garcia**, and **Randy A. Hall***
Department of Pharmacology, Emory University School of Medicine, Atlanta, GA, USA, 30322

Abstract

GPR37, also known as the parkin-associated endothelin-like receptor (Pael-R), is an orphan G protein-coupled receptor (GPCR) that exhibits poor plasma membrane expression when expressed in most cell types. We sought to find ways to enhance GPR37 trafficking to the cell surface in order to facilitate studies of GPR37 functional activity in heterologous cells. In truncation studies, we found that removing the GPR37 N-terminus (NT) dramatically enhanced the receptor's plasma membrane insertion. Further studies on sequential NT truncations revealed that removal of the first 210 amino acids increased surface expression nearly as much as removal of the entire NT. In studies examining the effects of co-expression of GPR37 with a variety of other GPCRs, we observed significant increases in GPR37 surface expression when the receptor was co-expressed with the adenosine receptor $A_{2A}R$ or the dopamine receptor D_2R. Co-immunoprecipitation experiments revealed that full-length GPR37 and, to a greater extent, the truncated GPR37 were capable of robustly associating with D_2R, resulting in modestly-altered D_2R affinity for both agonists and antagonists. In studies examining potential interactions of GPR37 with PDZ scaffolds, we observed a specific interaction between GPR37 and syntenin-1, which resulted in a dramatic increase in GPR37 surface expression in HEK-293 cells. These findings reveal three independent approaches – N-terminal truncation, co-expression with other receptors and co-expression with syntenin-1 – by which GPR37 surface trafficking in heterologous cells can be greatly enhanced to facilitate functional studies on this orphan receptor.

The orphan G-protein coupled receptor (GPCR) GPR37, also known as the parkin-associated endothelin-like receptor (Pael-R), is highly expressed in the mammalian central nervous system, but its function still remains largely unknown. GPR37 is most closely related to another CNS-enriched orphan receptor known as GPR37-like 1 (GPR37L1), and both orphans share significant sequence homology with the endothelin B receptor and other related peptide-activated GPCRs (1–5). However, none of the mammalian peptides tested so far, including endothelins, bombesin and others, have produced activation of any signaling pathways in heterologous cells or *Xenopus* oocytes expressing either GPR37 or GPR37L1 (2–5). A peptide called "head activator" (HA), which is derived from the freshwater coelenterate *Hydra*, has been reported to be capable of activating GPR37 (6), but no peptide equivalent to HA has been definitively identified in vertebrates. Thus, GPR37 and GPR37L1 must still be considered orphan GPCRs at the present time.

A major stumbling block impeding progress in understanding the ligand binding and signaling of GPR37 is the receptor's poor trafficking to the plasma membrane in most heterologous cell lines. GPR37 is commonly misfolded and therefore aggregated in the endoplasmic reticulum

[†]This work was supported by the Pharmacological Sciences training grant T32 GM008602, the NIH and the W.M. Keck Foundation.

*Address correspondence to: Randy A. Hall, Rollins Research Center, Rm 5113, 1510 Clifton Rd. Atlanta, GA, USA, 30322; Phone: 404-727-3699; Fax: 404-727-0365; rhall@pharm.emory.edu .

(ER) (1,7–9). The E3 ubiquitin ligase parkin ubiquitinates misfolded GPR37 in the ER, targeting it for degradation and thus preventing detrimental aggregation. Mutations to parkin, observed in post-mortem brain tissue of patients with autosomal recessive juvenile Parkinson's disease (AR-JP), inhibit proper functioning of parkin (1). It is believed that these mutations allow for aggregation of GPR37 along with other parkin substrates, leading to significant ER stress and eventually neuronal cell death (1,7–9). Additionally, GPR37 knockout (KO) mice are resistant to MPTP-induced neurotoxicity, a commonly-used animal model of Parkinson's disease (PD) (10). Moreover, autophagosome accumulations are found in brain samples of patients with PD, and recent findings suggest that overexpression of GPR37 can induce autophagy (9). These findings suggest that GPR37 may play a role in the pathology of PD, which enhances the importance of gaining insight into the trafficking and signaling of this orphan receptor.

Other GPCRs that exhibit trafficking defects in heterologous cells, including $GABA_BR1$ (11–15), the CB1 cannabinoid receptor (16), and the α_{1D}-adrenergic receptor (17–20), have been shown to be more efficiently trafficked following truncations of either the receptor's N-terminal (NT) or C-terminal (CT) regions (21). Thus, in the studies reported here, we created truncated forms of GPR37 to shed light on specific regions of GPR37 that influence its plasma membrane expression. Moreover, since interactions between GPCRs have been shown in some cases to strongly influence receptor surface expression and functional activity (21–25), we examined the capacity of GPR37 to associate with other GPCRs. Finally, because PDZ scaffolds have the capacity to affect surface expression of certain receptors (21,26), we examined the capacity of the GPR37 CT to interact with PDZ scaffold proteins. Our studies have revealed that removal of a portion of the GPR37 NT results in a dramatic enhancement of receptor surface expression, that co-expression with certain other receptors enhances GPR37 trafficking to the plasma membrane, and that interactions with the PDZ scaffold protein syntenin-1 promote GPR37 surface expression.

MATERIALS AND METHODS

Materials

Materials were obtained from the following sources: human embryonic kidney 293 (HEK-293) cells, ATCC (Manassas, VA); HA-A_{2A}R, HA-A_{2B}R, EE-$G\alpha_{i1}$, EE-$G\alpha_q$, GPR37, HA-NPY_1R, HA-NPY_2R, HA-D_2R, HA-D_1R, Missouri S&T cDNA Resource Center (Rolla, MO); FLAG-GPR37L1, Multispan (Hayward, CA); Dulbecco's modified Eagle medium (DMEM), Lipofectamine 2000, precast 4–20% Tris-Glycine gels, AlexaFluor 488 and 800 goat-anti-mouse antibodies, Alexa Fluor 546 and 700 goat-anti-rabbit antibodies, Invitrogen (Carlsbad, CA); anti-FLAG M2 monoclonal antibody, forskolin, isoproterenol, haloperidol, butaclamol, dopamine, (−)-quinpirole hydrochloride, cAMP, GDP, GTP, anti-FLAG M2-agarose, Sigma (St. Louis, MO); complete protease inhibitors, anti-HA 3F10 polyclonal antibody, anti-HA 12CA5 monoclonal antibody, Roche (Indianapolis, IN); DAPI, AppliChem (Ottoweg, Darmstadt, Germany); ECL™ anti-mouse IgG, Horseradish peroxidase-linked whole antibody, [^{3}H]-cAMP, [^{3}H]-spiperone, GE Healthcare (Buckhinghamshire, UK); anti-Na^+/K^+ ATPase antibody, Upstate/Millipore (Billerica, MA); penicillin-streptomycin solution, bovine serum albumin (BSA), ScintiSafe™ scintillation fluid, Fisher (Herndon, VA); fetal bovine serum (FBS), Atlanta Biologicals (Atlanta, GA); QuickChange XL site-directed mutagenesis kit, Stratagene (Cedar Creek, TX); head activator neuropeptide, Phoenix Pharmaceuticals (Belmont, CA) and Bachem AG (Bubendorf, Switzerland); SuperSignal Elisa Pico ECL reagent, Pierce (Rockford, IL); nitrocellulose membranes, Bio-Rad (Hercules, CA); Brandel Filters, Brandel Inc. (Gaithersburg, MD); p44/42 MAPK (ERK1/2) rabbit antibody and immobilized phsopho-p44/42 MAPK (ERK1/2) mouse antibody, Cell Signaling Technology (Danvers, MA); Brandel filters, Brandel Inc. (Gaithersburg, MD); [^{3}H]-

YM-019151-2, Perkin Elmer (Waltham, MA); [^{3}H]-adenine, [^{3}H]-adenosine, American Radiolabeled Chemicals, Inc. (St. Louis, MO)

Cell Culture and Transfection

HEK-293 cells were maintained in DMEM supplemented with 10% FBS and 1% penicillin-streptomycin solution at 37°C with 5% CO_2. Cells in 10-cm tissue culture dishes at a confluency of 50–60% were transfected with 1–3 μg of cDNA mixed with 15 μl Lipofectamine 2000 in 5ml of serum-free medium. Following a 4–5 h incubation, complete medium was added to stop the transfection. The cDNAs used were FLAG-GPR37 in pCMV2b, FLAG-GPR37L1 in pMEX2, ΔCT, $\Delta^{1–35}$, $\Delta^{1–70}$, $\Delta^{1–105}$, $\Delta^{1–140}$, $\Delta^{1–175}$, $\Delta^{1–210}$, and $\Delta^{1–255}$ FLAG-GPR37 in pCMV2b, 3×HA-D_2R, 3×HA-A_{2A} and A_{2B}R, EE-tagged $G\alpha_o$ and $G\alpha_q$ and HA-NPYRs 1 and 2 in pCDNA3.1 (+), DAT in pcDNA3.1 (−)/Neo, syntenin-1 in pMT-HA vector, and empty pCMV2b vector. All cDNAs used were human.

Surface Luminometer Assay

HEK-293 cells transiently transfected with FLAG-tagged or HA-tagged constructs were split into poly-D-lysine-coated 35-mm dishes and grown overnight at 37°C. For internalization assays, ligand was added into incomplete media and placed on cells for 30–60 min at 37°C. The cells were washed with phosphate-buffered saline (PBS + Ca^{2+}), fixed 30 min with 2% paraformaldehyde (PFA) and washed with PBS + Ca^{2+} again. The cells were then incubated in blocking buffer (2% nonfat dry milk in PBS, pH 7.4) for 30 min at room temperature (RT), followed by RT incubation with horseradish peroxidase-conjugated M2-anti-FLAG antibody (1:1000) or 12CA5-anti-HA antibody (1:1000) in blocking buffer for 1 h. For tracking HA-tagged receptors, cells were washed and incubated with anti-mouse IgG, horseradish peroxidase-linked whole antibody (1:2500) 30 min at RT. The cells were washed twice with blocking buffer, washed once with PBS + Ca^{2+}, and incubated with SuperSignal Pico ECL reagent for 15 s. Luminescence of the entire 35-mm dish was determined using a TD20/20 luminometer (Turner Designs).

Flow Cytometry

HEK-293 cells that had been transiently transfected were split into poly-D-lysine-coated 35-mm dishes and grown overnight at 37°C. The cells were transferred to ice, washed with PBS + Ca^{2+} once and incubated with M2 anti-FLAG antibody (1:300) in 1% BSA for 1 hour. Then, the cells were washed once and incubated in the dark with Alexa Fluor 488 anti-mouse antibody (1:500) in 1% BSA for 1 hour. Again, the cells were washed once, incubated for 15 minutes with 10mM Tris, 5mM EDTA, shaken loose, and transferred to tubes containing equal volume 4% PFA. Samples were spun down, supernatant aspirated, and resuspended in 250 μl 1% BSA. Flow cytometric acquisition and analysis were performed on at least 10,000 acquired events on an LSR II flow cytometer driven by FACSDiva software (BD Biosciences). Data analysis was performed using FlowJo software (Tree Star).

Mutagenesis

Six forward primers and one reverse primer were designed to make sequential truncations of GPR37. Truncated constructs were generated via PCR using those primers and a cDNA corresponding to full length GPR37. The PCR products were digested with BamHI and EcoRI and inserted into previously digested pCMV-2B, containing an N-terminal FLAG epitope. All sequences of truncated receptors were confirmed by sequence analysis (Agencourt, Beverly, MA).

Western Blotting

Samples were resolved by SDS-PAGE on 4–20% Tris-Glycine gels, followed by transfer to nitrocellulose membranes. The membranes were incubated in blocking buffer (2% nonfat dry milk, 50mM NaCl, 20mM HEPES, 0.1% Tween 20) for 30 min and then incubated with primary antibody for either 1 h at RT or overnight at 4°C. Next, the membranes were washed three times in blocking buffer and incubated with either a fluorescent- or HRP-conjugated secondary antibody for 30 min, washed three times more, and finally visualized using either the Odyssey imaging system (Li-Cor) or via ECL reagent followed by exposure to film.

Confocal Microscopy

Cells transiently transfected with FLAG-tagged constructs were grown on poly-D-lysine coated glass slides. The cells were rinsed with PBS+ Ca^{2+}, fixed with 2% PFA at RT, and washed 3 times with PBS+ Ca^{2+}. Fixed cells were permeabilized and blocked by incubating 30 min at RT in saponin buffer (1% BSA, 0.08% saponin, PBS+ Ca^{2+}). Next, the cells were washed 3 times and incubated with rabbit anti-FLAG antibody (1:1000) and anti-Na^{+}/K^{+} ATPase (1:500) in 1% BSA, 37° C for 1 h. After two times washing with PBS + Ca^{2+}, cells were incubated in the dark with Alexa Fluor anti-mouse 488 and anti-rabbit 546 antibodies (1:250) in 1% BSA for 1 hr at RT. Cells were washed 2 more times for 5 min with PBS + Ca^{2+}, DAPI-stained for 10 min, rinsed twice with water, and mounted with Vectashield mounting medium. Cells were examined using a Zeiss LSM 510 laser scanning confocal microscope. For MATLAB analysis, confocal images were saved as Photoshop files. The plasma membrane regions were then outlined, and a section of the background of each image was also outlined in order to be subtracted from the signal as non-specific binding. A MATLAB (Mathworks; Natick, MA) program was then used to analyze all cells to quantify the amount of receptor (red) on the cell surface (green).

Immunoprecipitation Studies

Transiently-transfected HEK-293 cells were harvested by washing once in ice-cold PBS and scraping in harvest buffer (10 mM HEPES, 100 mM NaCl, 5 mM EDTA, 1 mM benzamidine, protease inhibitor tablet, 1% Triton X-100, pH 7.4). Cell lysates were then solubilized, immunoprecipitated with anti-FLAG M2 affinity resin or protein A/G beads with anti-HA 3F10, and washed by repeated centrifugation and homogenization. Samples were heated, then probed via Western blotting using anti-FLAG M2 or anti-HA 3F10 antibodies.

Ligand Binding Studies

For preparation of cell lysates to be used in ligand binding assays, transfected cells grown on 100-mm dishes were rinsed with 2 ml PBS + Ca^{2+}, then starved for 1 hr in 5 ml PBS + Ca^{2+}. The cells were scraped into 1 ml of ice-cold binding buffer (20 mM HEPES, 100 mM NaCl, 5mM MgCl, 1.5 mM CaCl, 5mM KCl, 0.5mM EDTA, protease inhibitor tablet, pH 7.4). Cells were frozen at −20°C until use. On the day of the assay, cells were thawed and centrifuged at 13,500 rpm for 15 min to separate membranes. Membranes were then resuspended in 1 ml binding buffer, triturated, and incubated with increasing concentrations of unlabeled ligands in the presence of 0.5 nM [^{3}H]-spiperone to generate competition curves. The samples were incubated for one hour at 25°C. Nonspecific binding was defined as [^{3}H]-spiperone binding in the presence of 50 μM (+)-butaclamol, and represented less than 10% of total binding in all experiments. Incubations were terminated via filtration through GF/C filter paper, previously soaked in a 0.05% polyethylenemine solution, using a Brandel cell harvester. On the harvester, filters were rapidly washed three times with ice-cold wash buffer (10 mM HEPES, 50 mM NaCl), and radioactive ligand retained by the filters was quantified via liquid scintillation spectrometry. The fitting of curves for one site versus two sites was performed, and goodness

of fit was quantified using F tests, comparing sum-of-squares values for the one-site versus two-site fits.

Purification of Fusion Proteins

Wild type and mutant (removal of final cysteine) GST-tagged constructs (termed GPR37-CT and GPR37-Mut-CT, respectively) were created by PCR followed by insertion into the pGEX-4T1 vector. Overnight cultures of BL-21 DE Gold cells transformed with pGEX-4T1, pGEX4T-1CT or pGEX 4T-1Mut were diluted 1:143 into 1L of LB broth supplemented with appropriate antibiotics and grown to an optical density (A600) of 0.6–0.7 at 37°C. IPTG was then added to the culture and allowed to incubate for 2 h. Bacteria were pelleted by centrifugation, and the GST, GPR37-CT-GST, or GPR37-Mut-GST fusion proteins were purified using Sigma GSH agarose. The fusion proteins remained attached to GST agarose for the syntenin-1 pull-down or were eluted for use in overlays of the PDZ array. Eluted proteins were concentrated using the Amicon Ultra protein concentration system via centrifugation at 4°C to remove excess glutathione, and the concentration of the purified proteins were determined by QuickStart™ Bradford protein assay according to the manufacturer's protocols (Bio-Rad).

Fusion Protein Pull-down Assays

HEK-293 cells transiently transfected with HA-syntenin-1 (kindly provided by Paul Coffer, UMC Utrecht) were harvested in a detergent-free harvest buffer (10 mM HEPES, 50 mM NaCl, 5 mM EDTA, protease inhibitor tablet). The cells were spun down to isolate the membranes, which were then incubated in harvest buffer containing 1% Triton X-100 for 1h at 4°C with end-over-end agitation. The samples were spun down again to separate the soluble lysates from insoluble material. A sample of the solubilized protein was retained to ensure syntenin-1 expression and solubilization. The remaining lysates were divided evenly and incubated with glutathione agarose beads loaded with GST, GPR37-CT-GST, or GPR37-Mut-GST fusion proteins end-over-end for 1h at 4°C. The beads were washed 5 times with harvest buffer containing 1% Triton X-100 and then heated in sample buffer to strip proteins from the beads. The samples were then analyzed via Western blot for pull-down of syntenin-1 using an anti-HA antibody.

Statistical Analysis

All statistical analyses were carried out using Graph Pad Prism software (GraphPad Software Inc., San Diego, CA).

RESULTS

N-terminal truncation of GPR37 increases plasma membrane expression

HEK-293 cells were transfected with FLAG-tagged GPR37 (Fig. 1*A*) or GPR37L1 (Fig. 1*B*). Plasma membrane trafficking of the receptors was assessed using three independent techniques: a quantitative luminometer-based assay, FACS analysis, and confocal microscopy. In the luminometer-based surface expression assays, very little plasma membrane expression of GPR37 was observed, consistent with previous reports (1,6,8,27). In contrast, GPR37L1 was robustly trafficked to the plasma membrane (Fig. 1*C*). FACS analysis confirmed that GPR37L1 was highly expressed on the cell surface, whereas GPR37 expression was barely detectable (Fig. 1*D*) despite comparable levels of Western blot staining for the two receptors (data not shown). To confirm these findings via a third independent technique, confocal microscopy studies were performed using the Na^+/K^+ ATPase as a plasma membrane marker. As shown in the representative images in Figure 1, mainly punctate intracellular staining was observed for GPR37 (Fig. 1*E*), whereas GPR37L1 was predominantly localized at the plasma

membrane (Fig. 1*F*). MATLAB analysis of the images revealed that approximately 42% of the overall transfected GPR37L1 exhibited cell surface expression, whereas the cell surface expression for wt GPR37 was undetectable by these methods (<1%). Thus, despite the high degree of sequence similarity between the two receptors, GPR37L1 exhibited robust surface expression in our studies whereas GPR37 was poorly trafficked to the plasma membrane.

Given the striking difference in plasma membrane expression between GPR37 and GPR37L1, we next focused on determining which region of these related receptors might account for this difference. GPR37L1 shares 68% homology and 48% identity with GPR37, with most of the sequence identity concentrated in the receptors' transmembrane regions (3,5). Since the main differences between the two receptors are found in their diverging NT and CT sequences, we created two N-terminally FLAG-tagged truncated mutants of GPR37 – one in which 255 N-terminal amino acids were deleted (ΔNT-GPR37; Fig. 2*A*) and a second in which 58 C-terminal amino acids were deleted (ΔCT-GPR37; Fig. 2*B*). In the luminometer-based assay, the surface expression of ΔCT-GPR37 was observed to be equivalent to full-length GPR37, hereafter identified as wild-type GPR37 (wt GPR37). However, the ΔNT-GPR37 mutant exhibited a striking increase in surface expression relative to either of the other constructs (Fig. 2*C*). These findings were confirmed in flow cytometry experiments (Fig. 2*D*), as well as with confocal microscopy, in which ΔCT-GPR37 exhibited the same intracellular distribution as wt GPR37 (Fig. 2*E*), while ΔNT-GPR37 was predominantly associated with the plasma membrane (Fig. 2*F*). Again, MATLAB analysis confirmed the qualitative observations, with about 38% of transfected ΔNT-GPR37 expressing at the cell surface.

Regions of the GPR37 N-terminus control receptor surface expression

The results with the ΔNT-GPR37 mutant suggested that a motif on the GPR37 NT is a critical determinant of the plasma membrane localization of GPR37. To determine the location and sequence of this potential motif, we generated 6 sequentially truncated constructs of GPR37 – $\Delta^{1–35}$, $\Delta^{1–70}$, $\Delta^{1–105}$, $\Delta^{1–140}$, $\Delta^{1–175}$, and $\Delta^{1–210}$ GPR37– removing 35 more amino acids from the NT in each additional construct (Fig. 3*A*). Evaluation of the cell surface expression of these constructs was performed using the luminometer-based assay. As shown in Fig. 3*B*, very little surface expression was observed in the first 4 mutants, and the $\Delta^{1–175}$ mutant exhibited only a slight increase over wt GPR37. However, the $\Delta^{1–210}$ mutant exhibited a robust enhancement in cell surface expression, similar to that of ΔNT-GPR37. Confocal images revealing colocalization between $\Delta^{1–210}$ GPR37 and the Na^+/K^+ ATPase, a plasma membrane marker, confirmed the findings from the luminometer experiments (Fig. 3*C*); analysis of the images using MATLAB revealed that approximately 25% of the overall transfected $\Delta^{1–210}$ GPR37 exhibited cell surface expression.

The *Hydra* peptide head activator (HA) has been reported to be a ligand that activates and induces internalization of GPR37 in a pertussis-toxin sensitive manner, indicating that HA might promote GPR37 coupling to $G\alpha_i$ or $G\alpha_o$ (6). To test if the GPR37 mutants that exhibited enhanced trafficking, ΔNT-GPR37 and $\Delta^{1–210}$ GPR37, also exhibited functional activity in response to HA peptide, HEK-293 cells were transfected with either ΔNT, $\Delta^{1–210}$ or wt GPR37 and then stimulated with HA. Luminometer-based surface expression assays were performed to measure HA-induced receptor internalization, phospho-ERK assays were performed to assess HA-stimulated ERK1/2 phosphorylation, and cyclic AMP assays were carried out to test for HA-induced inhibition of adenylyl cyclase activity. However, despite repeated studies with HA peptide from different sources and examined over a range of concentrations, we were unable to find evidence for HA-induced activation of ΔNT, $\Delta^{1–210}$ or wt GPR37 in these studies (data not shown).

Dopamine receptor D_2R interacts with GPR37

Studies of other poorly trafficked GPCRs, such as the aforementioned $GABA_BR1$ and α_{1D}-AR, have revealed that receptor surface expression can sometimes be greatly enhanced upon co-expression with interacting GPCRs (21–25). GPR37 has been reported to associate with the dopamine transporter (DAT) (28), but there have not yet been any studies of possible GPR37 interactions with other GPCRs. Thus, we co-expressed GPR37 in HEK-293 cells with DAT, as well as a handful of GPCRs that possess similar regional expression patterns in the brain, and quantified GPR37 surface expression. In comparison with GPR37 expressed alone, the luminometer-based cell surface assay revealed an increase in GPR37 surface expression when co-expressed with the adenosine A_{2A} receptor, as well as a much larger increase when co-expressed with dopamine D_2R (Fig. 4*A*). Neither DAT nor any of the other receptors ($A_{2B}R$ and neuropeptide receptors NPY_1 and NPY_2) had any effect on surface expression of GPR37. To examine whether D_2R might form complexes with GPR37 in cells, we performed co-immunoprecipitation studies, which revealed a robust interaction between GPR37 and D_2R (Fig. 4*B–E*). Both wt GPR37 (Fig. 4*D*) and the $\Delta^{1–210}$ mutant (Fig. 4*E*) co-immunoprecipitated with both the immature (unprocessed) and mature (glycosylated) forms of D_2R (lower and upper bands, respectively), indicating the interaction between these two receptors likely occurs in the ER and is maintained after glycosylation. The $\Delta^{1–210}$ mutant exhibited a consistently stronger interaction with D_2R than did wt GPR37, probably due to the enhanced plasma membrane expression of the mutant receptor. Therefore, we used the $\Delta^{1–210}$ mutant for further studies on the effects of GPR37 on D_2R properties.

Receptor-receptor interactions often modulate the endocytic trafficking of GPCRs (22–25). In some cases, interaction with a partner receptor can inhibit normal agonist-induced internalization of a given GPCR, whereas in other cases, stimulation by the ligand of one receptor can induce an interacting receptor to be co-internalized (29–31). To observe the effects of $\Delta^{1–210}$ GPR37 co-expression on the agonist-induced internalization rate of D_2R, and also to assess the possibility of $\Delta^{1–210}$ GPR37 co-internalization upon D_2R agonist stimulation, luminometer-based surface expression assays were carried out. Upon treatment with the D_2R agonist quinpirole for 30 minutes, the individually expressed D_2R internalized by 32 ± 9%. Similarly, when co-expressed with $\Delta^{1–210}$ GPR37 quinpirole-stimulated D_2R internalized by 33 ± 2%. Co-internalization of $\Delta^{1–210}$ GPR37 was not observed upon co-expression with D_2R and quinpirole stimulation, and co-immunoprecipitation experiments performed in the absence and presence of quinpirole treatment revealed that the interaction between D_2R and GPR37 was unchanged upon agonist stimulation (data not shown). Thus, we found no evidence for agonist regulation of the interaction, and also no evidence that the interaction altered agonist-promoted internalization of D_2R.

Co-expression with $\Delta^{1–210}$ GPR37 alters D_2R ligand-binding properties

To determine if the physical interaction between GPR37 and D_2R might have effects on D_2R functionality, ligand binding studies were performed using radiolabeled versions of the D_2R antagonists spiperone and YM-09151. Both ligands exhibited modest but significant increases in affinity for D_2R when D_2R was co-expressed with $\Delta^{1–210}$ GPR37 (Table 1). Competition curves were also performed for displacement of [^{3}H]-spiperone binding by unlabeled versions of the D_2R agonists dopamine and quinpirole and the D_2R antagonist haloperidol. The affinities of these ligands for D_2R were also somewhat altered when D_2R was co-expressed with $\Delta^{1–210}$ GPR37, with the magnitude of the change being ligand-specific (Table 1). To investigate whether these differences in ligand binding might correspond to changes in functional activity, [^{35}S]-GTPγS binding studies were performed on membranes derived from cells over-expressing $G\alpha_o$ protein and D_2R in the absence and presence of $\Delta^{1–210}$ GPR37. However, no significant shift in EC_{50} was observed when $\Delta^{1–210}$ GPR37 was co-expressed with D_2R, compared to D_2R alone (data not shown).

Co-expression of GPR37 with syntenin-1 enhances GPR37 surface expression

The GPR37 CT possesses a consensus Class 1 PDZ domain-binding motif (G-T-H-C). To examine whether GPR37 might interact via this motif with PDZ domain-containing scaffold proteins, we prepared the GPR37 CT as a GST fusion protein and screened it against a proteomic array of 96 purified PDZ domains (32,33). However, the GPR37-CT-GST fusion protein did not exhibit detectable binding to any of the PDZ domains on the array (data not shown). In addition to this proteomic approach toward searching for GPR37-interacting partners, we also took a bioinformatics approach and noted that GPR37 terminates in precisely the same C-terminal motif as the glycine transporter GlyT2 (G-T-x-C). Since GlyT2 has been shown to interact via this motif with the atypical PDZ scaffold syntenin-1 (34,35), which is not included in our array, we specifically examined whether GPR37 and syntenin-1 might interact. As shown in Figure 5A, pull-down analyses revealed a robust interaction between the GPR37-CT-GST and syntenin-1. This interaction was not seen using a mutated version of the GPR37-CT-GST protein (GPR37-Mut-GST), in which the final cysteine residue had been removed to disrupt the PDZ-binding motif. Moreover, when syntenin-1 was co-expressed with full-length GPR37 in HEK-293 cells, the result was a striking 10-fold increase in the amount of GPR37 that could be detected in the plasma membrane (Fig. 5*B*). Interestingly, co-expression of syntenin-1 with Δ^{1-210} GPR37 still resulted in a three-fold increase in the surface expression of the truncated mutant receptor, revealing that a combination of approaches (truncation of the receptor's NT and co-expression of the receptor with a CT-binding partner) can work synergistically to maximize GPR37 trafficking to the plasma membrane in heterologous cells (Fig. 5*B*).

DISCUSSION

Most GPCRs must reach the plasma membrane in order to achieve proper functional activity. Thus, the identification of ligands for orphan GPCRs can be greatly impeded if the receptors exhibit trafficking defects when expressed in heterologous cells. For this reason, we sought to find ways to enhance the surface trafficking of GPR37, an orphan receptor that is well-known to suffer from trafficking defects upon heterologous expression (1,6,8,27). We have identified three distinct approaches by which GPR37 trafficking to the plasma membrane can be enhanced: truncation of the receptor's N-terminus, co-expression with certain GPCRs, and co-expression with the PDZ scaffold syntenin-1.

The effects of truncating the GPR37 N-terminus are similar to the effects of N-terminal truncations on the surface trafficking of the CB1 cannabinoid receptor (16,36) and α_{1D}-adrenergic receptor (17–20). For both of these receptors, N-terminal truncations greatly improve receptor surface expression, although it is not certain if the receptors' N-termini possess specific ER retention motifs that are removed by the truncations or if instead there are global difficulties in folding that get resolved through the removal of hard-to-fold regions. It is unlikely that removal of glycosylation sites could account for the observed effects of N-terminal truncation in our studies, since removal of glycosylation sites almost invariably causes impairment in the surface expression of GPCRs rather than enhancement (37–40). Indeed, there are three putative sites of N-linked glycosylation sites on the NT of GPR37, but none of these sites is found between amino acids 175–210, which we determined to be the critical region for determining the receptor's surface expression.

After observing that N-terminal truncations could greatly enhance GPR37 surface trafficking in heterologous cells, we sought to determine if the surface-expressed truncated mutant versions of GPR37 were functionally active. Since the *Hydra* peptide head activator (HA) has been reported to be an agonist for GPR37, we explored potential HA-mediated stimulation of wt GPR37 and the truncated versions of GPR37. However, in a variety of assays under a variety of different conditions, we were unable to detect any evidence for HA-induced activation of

GPR37, GPR37L1 or any of the mutant versions of GPR37 that we had created. It is possible, of course, that truncations to the GPR37 N-terminus might destroy the binding site for HA, but comparable N-terminal truncations to the endothelin B receptor, the most closely-related receptor to GPR37 and GPR37L1, do not disrupt ligand binding (41,42). Thus, there is reason to believe that the truncated GPR37 mutants still may be functionally active. As for our studies on full-length GPR37, the discrepancy between the positive findings of Rezgaoui *et al*. (6) and our negative findings for HA stimulation of wild-type GPR37 might be explained by differences in the cell lines used or other technical factors. Regardless of the explanation, it seems that GPR37 and GPR37L1 should still be considered as orphan receptors at the present time, especially since it is not clear that a peptide similar to HA exists in vertebrates. Though there were a handful of papers several decades ago reporting HA-like immunoreactivity in sections of mammalian brains (43–45), there have not been any positive follow-up studies in the past twenty years to confirm these early observations.

In addition to truncations to the GPR37 N-terminus, we found a second approach that resulted in enhanced GPR37 surface expression in heterologous cells – co-expression with certain other GPCRs, notably the dopamine D_2 receptor and adenosine A_{2A} receptor. Interestingly, D_2R and $A_{2A}R$ are known to be capable of functional interactions with each other and are also known to be found abundantly in the striatum (46), a brain region where GPR37 is highly expressed (2,47). Many studies on cross-talk between D_2R and $A_{2A}R$ have focused on how stimulation of one of the receptors can directly influence the properties of the other partner (46). However, in the absence of a functional ligand for GPR37, such cross-talk studies on the putative heterodimers consisting of GPR37/D_2R and GPR37/$A_{2A}R$ are not possible at the present time. Thus, we focused on determining whether co-expression with GPR37 might alter D_2R properties.

In ligand binding studies, we found that co-expression with GPR37 induced modest shifts in the affinity of D_2R for various ligands. Although these shifts were only in the range of 1.5-to 2.5-fold, the true magnitude of the changes may be underestimated in our studies, since our transfection efficiency was not 100%. Moreover, it is unlikely that there would be 100% efficient co-assembly of the receptors even in cells that were doubly-transfected with D_2R and GPR37. Thus, any observed changes in the properties of the D_2R/GPR37 heterodimer relative to D_2R alone would likely be underestimated in co-expression studies of this type. As for the potential *in vivo* relevance of the GPR37 effects on D_2R properties, it is interesting to note that the affinity of D_2R for [^{3}H]-YM-09151-2 in GPR37 knockout mice is decreased by approximately two-fold (28), which is strikingly consistent with the approximately two-fold increase in D_2R affinity for [^{3}H]-YM-09151-2 that we observed upon co-transfection of D_2R with GPR37. If it is true that associations between GPR37 and D_2R can subtly influence D_2R antagonist binding properties *in vivo*, this is a point of significant clinical interest given the widespread use of D_2R antagonists in treating schizophrenia (48). Since GPR37 is co-expressed *in vivo* with D_2R in some neuronal populations but not others (47), it may be possible to develop D_2R antagonists with enhanced regional selectivity by developing compounds that preferentially target the D_2R/GPR37 complex relative to D_2R alone (or vice versa).

The third and final approach that we found to result in enhanced surface expression of GPR37 was co-expression with the PDZ scaffold syntenin-1. These findings are similar to previous observations that surface trafficking of the α_{1D}-adrenergic receptor can be strongly promoted by receptor interactions with a distinct class of PDZ scaffolds, the syntrophins (49,50). The interaction of GPR37 with syntenin-1 was quite specific, as screens of a proteomic array consisting of 96 other PDZ domains with the GPR37-CT did not reveal detectable interactions with any other PDZ domains. GPR37 terminates in a motif, G-T-x-C, that is identical to the motif found at the C-terminus of the syntenin-1 binding partner GlyT2 (34,35). For GlyT2, the primary functional consequence of interaction with syntenin-1 is enhanced trafficking to

synapses (35). For several other syntenin-1-interacting proteins, including pro-transforming growth factor α (51), CD63 (52) and the Notch ligand Delta1 (53), co-expression with syntenin-1 has been shown to markedly enhance trafficking to the plasma membrane, similar to the effects on GPR37 that we observed in our studies. Interestingly, syntenin-1 is known to be highly expressed in oligodendrocytes (54), the cell type in which GPR37 is most abundantly expressed (1). Since GPR37 is an orphan receptor, it is not possible at the present time to test whether the GPR37/syntenin-1 association has effects on the receptor's functional properties, but the dramatic effects of syntenin-1 on GPR37 surface expression may prove useful in screens for potential GPR37 ligands that would allow for deorphanization of the receptor.

In summary, we have elucidated three distinct approaches by which the trafficking of GPR37 to the plasma membrane can be enhanced. Moreover, we have shown that GPR37L1, a close relative of GPR37, exhibits robust surface expression in heterologous cells. Thus, if it is assumed that GPR37 and GPR37L1 are activated by the same ligand, or at least related ligands, it seems that GPR37L1 might prove the superior choice for screens attempting to identify the ligand(s) for this orphan receptor pair. However, screens focused solely on GPR37 may benefit from application of one or several of the approaches described here, including N-terminal truncation, co-expression with partner receptors and/or co-expression with syntenin-1, in order to achieve improved surface trafficking and enhanced functionality of GPR37. Furthermore, when more is known about the ligand binding and signaling capabilities of GPR37, the interactions described here between GPR37 and other receptors and GPR37/syntenin-1 may eventually help to shed light on the regulation of GPR37 functional activity *in vivo*.

Abbreviations

Pael-R, parkin-associated endothelin-like receptor
GPCR, G-protein coupled receptor
NT, N-terminus
HA, head activator
ER, endoplasmic reticulum
AR-JP, autosomal recessive juvenile Parkinson's disease
KO, knockout
PD, Parkinson's disease
CT, C-terminal
wt, wild-type
GST, glutathione *S*-transferase
HEK, human embryonic kidney
PFA, paraformaldehyde
BSA, bovine serum albumin
FBS, fetal bovine serum

Acknowledgments

We would like to thank Heide Oller for her help in the construction of several constructs used in these studies. We also would like to thank Howard Rees for his guidance with the confocal microscope, Richard Dunham for his help with flow cytometry and Cristina Bush for her assistance with the luminometer-based surface assays. In addition, we want to thank Paul Coffer for providing the HA-syntenin-1 construct, Gary Miller for the DAT construct, and Daniela Marazziti for her suggestions, guidance and discussion.

Reference List

1. Imai Y, Soda M, Inoue H, Hattori N, Mizuno Y, Takahashi R. An unfolded putative transmembrane polypeptide, which can lead to endoplasmic reticulum stress, is a substrate of Parkin. Cell 2001;105:891–902. [PubMed: 11439185]

2. Zeng Z, Su K, Kyaw H, Li Y. A novel endothelin receptor type-B-like gene enriched in the brain. Biochem Biophys Res Commun 1997;233:559–567. [PubMed: 9144577]
3. Leng N, Gu G, Simerly RB, Spindel ER. Molecular cloning and characterization of two putative G protein-coupled receptors which are highly expressed in the central nervous system. Brain Res Mol Brain Res 1999;69:73–83. [PubMed: 10350639]
4. Marazziti D, Golini E, Gallo A, Lombardi MS, Matteoni R, Tocchini-Valentini GP. Cloning of GPR37, a gene located on chromosome 7 encoding a putative G-protein-coupled peptide receptor, from a human frontal brain EST library. Genomics 1997;45:68–77. [PubMed: 9339362]
5. Valdenaire O, Giller T, Breu V, Ardati A, Schweizer A, Richards JG. A new family of orphan G protein-coupled receptors predominantly expressed in the brain. FEBS Lett 1998;424:193–196. [PubMed: 9539149]
6. Rezgaoui M, Susens U, Ignatov A, Gelderblom M, Glassmeier G, Franke I, Urny J, Imai Y, Takahashi R, Schaller HC. The neuropeptide head activator is a high-affinity ligand for the orphan G-protein-coupled receptor GPR37. J Cell Sci 2006;119:542–549. [PubMed: 16443751]
7. Imai Y, Soda M, Hatakeyama S, Akagi T, Hashikawa T, Nakayama KI, Takahashi R. CHIP is associated with Parkin, a gene responsible for familial Parkinson's disease, and enhances its ubiquitin ligase activity. Mol Cell 2002;10:55–67. [PubMed: 12150907]
8. Kubota K, Niinuma Y, Kaneko M, Okuma Y, Sugai M, Omura T, Uesugi M, Uehara T, Hosoi T, Nomura Y. Suppressive effects of 4-phenylbutyrate on the aggregation of Pael receptors and endoplasmic reticulum stress. J Neurochem 2006;97:1259–1268. [PubMed: 16539653]
9. Marazziti D, Di Pietro C, Golini E, Mandillo S, Matteoni R, Tocchini-Valentini GP. Induction of macroautophagy by overexpression of the Parkinson's disease-associated GPR37 receptor. FASEB J. 2009
10. Marazziti D, Golini E, Mandillo S, Magrelli A, Witke W, Matteoni R, Tocchini-Valentini GP. Altered dopamine signaling and MPTP resistance in mice lacking the Parkinson's disease-associated GPR37/parkin-associated endothelin-like receptor. Proc Natl Acad Sci U S A 2004;101:10189–10194. [PubMed: 15218106]
11. Couve A, Filippov AK, Connolly CN, Bettler B, Brown DA, Moss SJ. Intracellular retention of recombinant GABAB receptors. J Biol Chem 1998;273:26361–26367. [PubMed: 9756866]
12. Calver AR, Robbins MJ, Cosio C, Rice SQ, Babbs AJ, Hirst WD, Boyfield I, Wood MD, Russell RB, Price GW, Couve A, Moss SJ, Pangalos MN. The C-terminal domains of the GABA(b) receptor subunits mediate intracellular trafficking but are not required for receptor signaling. J Neurosci 2001;21:1203–1210. [PubMed: 11160390]
13. Margeta-Mitrovic M, Jan YN, Jan LY. A trafficking checkpoint controls GABA(B) receptor heterodimerization. Neuron 2000;27:97–106. [PubMed: 10939334]
14. Margeta-Mitrovic M, Mitrovic I, Riley RC, Jan LY, Basbaum AI. Immunohistochemical localization of GABA(B) receptors in the rat central nervous system. J Comp Neurol 1999;405:299–321. [PubMed: 10076927]
15. Pagano A, Rovelli G, Mosbacher J, Lohmann T, Duthey B, Stauffer D, Ristig D, Schuler V, Meigel I, Lampert C, Stein T, Prezeau L, Blahos J, Pin J, Froestl W, Kuhn R, Heid J, Kaupmann K, Bettler B. C-terminal interaction is essential for surface trafficking but not for heteromeric assembly of GABA(b) receptors. J Neurosci 2001;21:1189–1202. [PubMed: 11160389]
16. Andersson H, D'Antona AM, Kendall DA, Von Heijne G, Chin CN. Membrane assembly of the cannabinoid receptor 1: impact of a long N-terminal tail. Mol Pharmacol 2003;64:570–577. [PubMed: 12920192]
17. Hague C, Chen Z, Pupo AS, Schulte NA, Toews ML, Minneman KP. The N terminus of the human alpha1D-adrenergic receptor prevents cell surface expression. J Pharmacol Exp Ther 2004;309:388–397. [PubMed: 14718583]
18. Hague C, Uberti MA, Chen Z, Hall RA, Minneman KP. Cell surface expression of alpha1D-adrenergic receptors is controlled by heterodimerization with alpha1B-adrenergic receptors. J Biol Chem 2004;279:15541–15549. [PubMed: 14736874]
19. Pupo AS, Uberti MA, Minneman KP. N-terminal truncation of human alpha1D-adrenoceptors increases expression of binding sites but not protein. Eur J Pharmacol 2003;462:1–8. [PubMed: 12591089]

20. Uberti MA, Hall RA, Minneman KP. Subtype-specific dimerization of alpha 1-adrenoceptors: effects on receptor expression and pharmacological properties. Mol Pharmacol 2003;64:1379–1390. [PubMed: 14645668]
21. Dunham JH, Hall RA. Enhancement of the surface expression of G protein-coupled receptors. Trends Biotechnol 2009;27:541–545. [PubMed: 19679364]
22. Prinster SC, Hague C, Hall RA. Heterodimerization of g protein-coupled receptors: specificity and functional significance. Pharmacol Rev 2005;57:289–298. [PubMed: 16109836]
23. Bulenger S, Marullo S, Chen Z, Bouvier M. Emerging role of homo- and heterdimerization in G-protein-coupled receptor biosynthesis and maturation. Trends Pharmacol Sci 2005;26:131–137. [PubMed: 15749158]
24. Ferre S, Quiroz C, Woods AS, Cunha R, Popoli P, Ciruela F, Lluis C, Franco R, Azdad K, Schiffmann SN. An update on adenosine A2A-dopamine D2 receptor interactions: implications for the function of G protein-coupled receptors. Curr Pharm Des 2008;14:1468–1474. [PubMed: 18537670]
25. Milligan G. G protein-coupled receptor hetero-dimerization: contribution to pharmacology and function. Br J Pharmacol 2009;158:5–14. [PubMed: 19309353]
26. Weinman EJ, Hall RA, Friedman PA, Liu-Chen LY, Shenolikar S. The association of NHERF adaptor proteins with g protein-coupled receptors and receptor tyrosine kinases. Annu Rev Physiol 2006;68:491–505. [PubMed: 16460281]
27. Yang Y, Nishimura I, Imai Y, Takahashi R, Lu B. Parkin suppresses dopaminergic neuron-selective neurotoxicity induced by Pael-R in Drosophila. Neuron 2003;37:911–924. [PubMed: 12670421]
28. Marazziti D, Mandillo S, Di Pietro C, Golini E, Matteoni R, Tocchini-Valentini GP. GPR37 associates with the dopamine transporter to modulate dopamine uptake and behavioral responses to dopaminergic drugs. Proc Natl Acad Sci U S A 2007;104:9846–9851. [PubMed: 17519329]
29. He L, Fong J, von Zastrow M, Whistler JL. Regulation of opioid receptor trafficking and morphine tolerance by receptor oligomerization. Cell 2002;108:271–282. [PubMed: 11832216]
30. Lavoie C, Mercier JF, Salahpour A, Umapathy D, Breit A, Villeneuve LR, Zhu WZ, Xiao RP, Lakatta EG, Bouvier M, Hebert TE. Beta 1/beta 2-adrenergic receptor heterodimerization regulates beta 2-adrenergic receptor internalization and ERK signaling efficacy. J Biol Chem 2002;277:35402–35410. [PubMed: 12140284]
31. Uberti MA, Hague C, Oller H, Minneman KP, Hall RA. Heterodimerization with beta2-adrenergic receptors promotes surface expression and functional activity of alpha1D-adrenergic receptors. J Pharmacol Exp Ther 2005;313:16–23. [PubMed: 15615865]
32. Fam SR, Paquet M, Castleberry AM, Oller H, Lee CJ, Traynelis SF, Smith Y, Yun CC, Hall RA. P2Y1 receptor signaling is controlled by interaction with the PDZ scaffold NHERF-2. Proc Natl Acad Sci U S A 2005;102:8042–8047. [PubMed: 15901899]
33. He J, Bellini M, Inuzuka H, Xu J, Xiong Y, Yang X, Castleberry AM, Hall RA. Proteomic analysis of beta1-adrenergic receptor interactions with PDZ scaffold proteins. J Biol Chem 2006;281:2820–2827. [PubMed: 16316992]
34. Ohno K, Koroll M, El Far O, Scholze P, Gomeza J, Betz H. The neuronal glycine transporter 2 interacts with the PDZ domain protein syntenin-1. Mol Cell Neurosci 2004;26:518–529. [PubMed: 15276154]
35. Armsen W, Himmel B, Betz H, Eulenburg V. The C-terminal PDZ-ligand motif of the neuronal glycine transporter GlyT2 is required for efficient synaptic localization. Mol Cell Neurosci 2007;36:369–380. [PubMed: 17851090]
36. Nordstrom R, Andersson H. Amino-terminal processing of the human cannabinoid receptor 1. J Recept Signal Transduct Res 2006;26:259–267. [PubMed: 16818376]
37. He J, Xu J, Castleberry AM, Lau AG, Hall RA. Glycosylation of beta(1)-adrenergic receptors regulates receptor surface expression and dimerization. Biochem Biophys Res Commun 2002;297:565–572. [PubMed: 12270132]
38. Alkenv M, Schmidt A, Rutz C, Furkert J, Kleinau G, Rosenthal W, Schulein R. The sequence after the signal peptide of the G protein-coupled endothelin B receptor is required for efficient translocon gating at the endoplasmic reticulum membrane. Mol Pharmacol 2009;75:801–811. [PubMed: 19136571]

39. Deslauriers B, Ponce C, Lombard C, Larguier R, Bonnafous JC, Marie J. N-glycosylation requirements for the AT1a angiotensin II receptor delivery to the plasma membrane. Biochem J 1999;339(Pt 2):397–405. [PubMed: 10191272]
40. Davis D, Liu X, Segaloff DL. Identification of the sites of N-linked glycosylation on the follicle-stimulating hormone (FSH) receptor and assessment of their role in FSH receptor function. Mol Endocrinol 1995;9:159–170. [PubMed: 7776966]
41. Klammt C, Srivastava A, Eifler N, Junge F, Beyermann M, Schwarz D, Michel H, Doetsch V, Bernhard F. Functional analysis of cell-free-produced human endothelin B receptor reveals transmembrane segment 1 as an essential area for ET-1 binding and homodimer formation. FEBS J 2007;274:3257–3269. [PubMed: 17535295]
42. Doi T, Hiroaki Y, Arimoto I, Fujiyoshi Y, Okamoto T, Satoh M, Furuichi Y. Characterization of human endothelin B receptor and mutant receptors expressed in insect cells. Eur J Biochem 1997;248:139–148. [PubMed: 9310371]
43. Bodenmuller H, Schaller HC. Conserved amino acid sequence of a neuropeptide, the head activator, from coelenterates to humans. Nature 1981;293:579–580. [PubMed: 7290191]
44. Bodenmuller H, Schaller HC, Darai G. Human hypothalamus and intestine contain a hydra-neuropeptide. Neurosci Lett 1980;16:71–74. [PubMed: 7052424]
45. Ekman R, Salford L, Brun A, Larsson I. Hydra head activator-like immunoreactivity in human brain astrocytomas grade III–IV and the surrounding brain tissue. Peptides 1990;11:271–275. [PubMed: 2162530]
46. Fuxe K, Ferre S, Genedani S, Franco R, Agnati LF. Adenosine receptor-dopamine receptor interactions in the basal ganglia and their relevance for brain function. Physiol Behav 2007;92:210–217. [PubMed: 17572452]
47. Lein ES, Hawrylycz MJ, Ao N, Ayres M, Bensinger A, Bernard A, Boe AF, Boguski MS, Brockway KS, Byrnes EJ, Chen L, Chen TM, Chin MC, Chong J, Crook BE, Czaplinska A, Dang CN, Datta S, Dee NR, Desaki AL, Desta T, Diep E, Dolbeare TA, Donelan MJ, Dong HW, Dougherty JG, Duncan BJ, Ebbert AJ, Eichele G, Estin LK, Faber C, Facer BA, Fields R, Fischer SR, Fliss TP, Frensley C, Gates SN, Glattfelder KJ, Halverson KR, Hart MR, Hohmann JG, Howell MP, Jeung DP, Johnson RA, Karr PT, Kawal R, Kidney JM, Knapik RH, Kuan CL, Lake JH, Laramee AR, Larsen KD, Lau C, Lemon TA, Liang AJ, Liu Y, Luong LT, Michaels J, Morgan JJ, Morgan RJ, Mortrud MT, Mosqueda NF, Ng LL, Ng R, Orta GJ, Overly CC, Pak TH, Parry SE, Pathak SD, Pearson OC, Puchalski RB, Riley ZL, Rockett HR, Rowland SA, Royall JJ, Ruiz MJ, Sarno NR, Schaffnit K, Shapovalova NV, Sivisay T, Slaughterbeck CR, Smith SC, Smith KA, Smith BI, Sodt AJ, Stewart NN, Stumpf KR, Sunkin SM, Sutram M, Tam A, Teemer CD, Thaller C, Thompson CL, Varnam LR, Visel A, Whitlock RM, Wohnoutka PE, Wolkey CK, Wong VY, Wood M, Yaylaoglu MB, Young RC, Youngstrom BL, Yuan XF, Zhang B, Zwingman TA, Jones AR. Genome-wide atlas of gene expression in the adult mouse brain. Nature 2007;445:168–176. [PubMed: 17151600]
48. Strange PG. Antipsychotic drug action: antagonism, inverse agonism or partial agonism. Trends Pharmacol Sci 2008;29:314–321. [PubMed: 18471899]
49. Lyssand JS, DeFino MC, Tang XB, Hertz AL, Feller DB, Wacker JL, Adams ME, Hague C. Blood pressure is regulated by an alpha1D-adrenergic receptor/dystrophin signalosome. J Biol Chem 2008;283:18792–18800. [PubMed: 18468998]
50. Chen Z, Hague C, Hall RA, Minneman KP. Syntrophins regulate alpha1D-adrenergic receptors through a PDZ domain-mediated interaction. J Biol Chem 2006;281:12414–12420. [PubMed: 16533813]
51. Fernandez-Larrea J, Merlos-Suarez A, Urena JM, Baselga J, Arribas J. A role for a PDZ protein in the early secretory pathway for the targeting of proTGF-alpha to the cell surface. Mol Cell 1999;3:423–433. [PubMed: 10230395]
52. Latysheva N, Muratov G, Rajesh S, Padgett M, Hotchin NA, Overduin M, Berditchevski F. Syntenin-1 is a new component of tetraspanin-enriched microdomains: mechanisms and consequences of the interaction of syntenin-1 with CD63. Mol Cell Biol 2006;26:7707–7718. [PubMed: 16908530]
53. Estrach S, Legg J, Watt FM. Syntenin mediates Delta1-induced cohesiveness of epidermal stem cells in culture. J Cell Sci 2007;120:2944–2952. [PubMed: 17666427]

54. Chatterjee N, Stegmuller J, Schatzle P, Karram K, Koroll M, Werner HB, Nave KA, Trotter J. Interaction of syntenin-1 and the NG2 proteoglycan in migratory oligodendrocyte precursor cells. J Biol Chem 2008;283:8310–8317. [PubMed: 18218632]

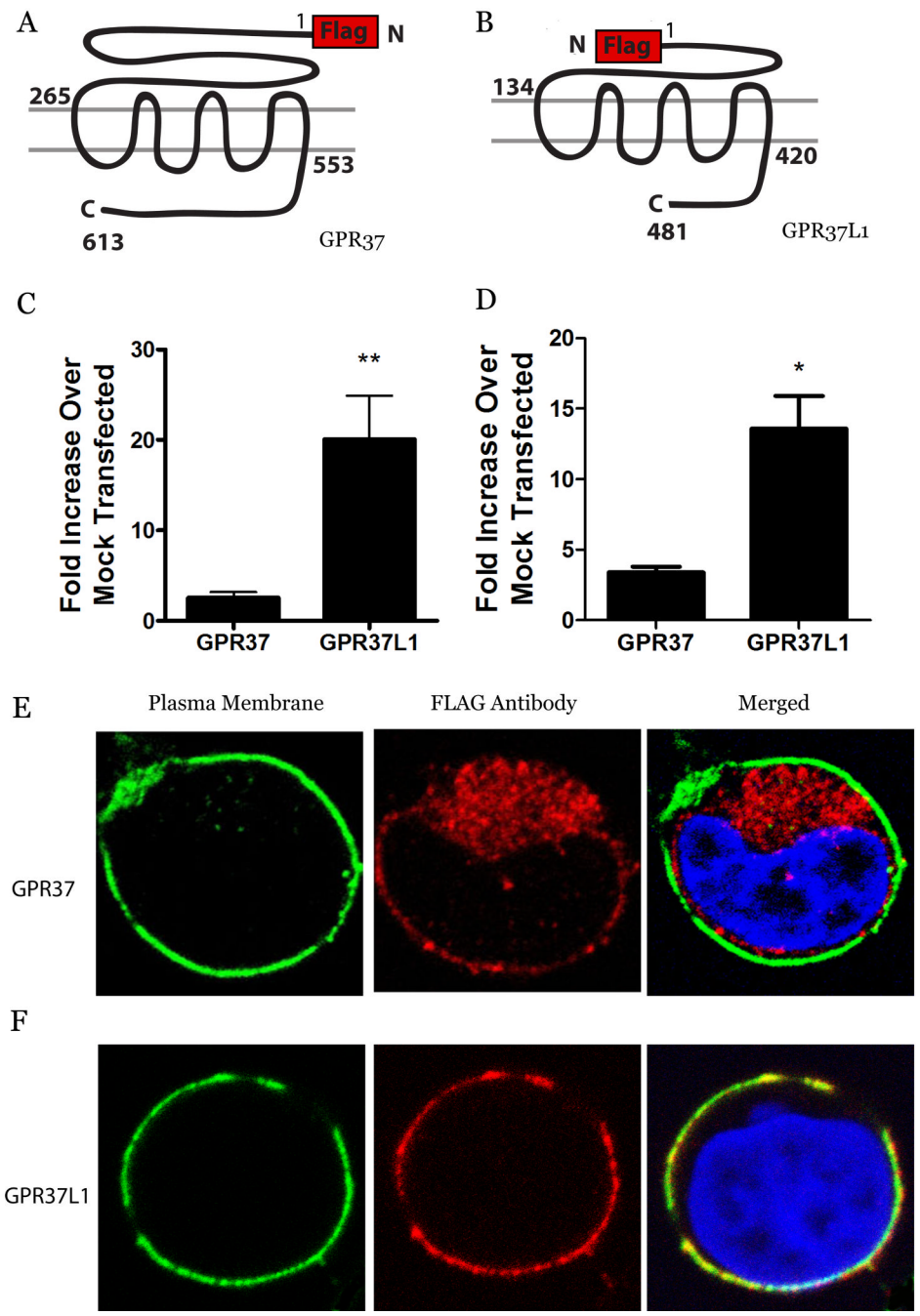

Fig. 1.

GPR37L1 exhibits robust plasma membrane expression but GPR37 does not. GPR37 (*A*) and GPR37L1 (*B*) were transiently transfected into HEK-293 cells. Cell surface expression was determined using a luminometer based assay (*C*) and via flow cytometry (*D*). Values are expressed as mean ± SEM for fold surface expression over mock transfected cells. Unpaired *t* tests were used to determine statistical significance ($n = 27$ & 3, respectively; *, $p < 0.05$, **, $p<0.005$). Confocal imaging of representative cells transfected with wt GPR37 (*E*) or GPR37L1 (*F*) was done using mouse anti-Na^+/K^+ ATPase, followed by Alexa-Fluor 488, to mark the cell surface (green, left panels), rabbit anti-FLAG, followed by Alexa-Fluor 546, to detect the

receptors (red, center panels), and DAPI to stain the nucleus (blue, right panels). Yellow indicates colocalization of receptor with plasma membrane (C&D, right panels).

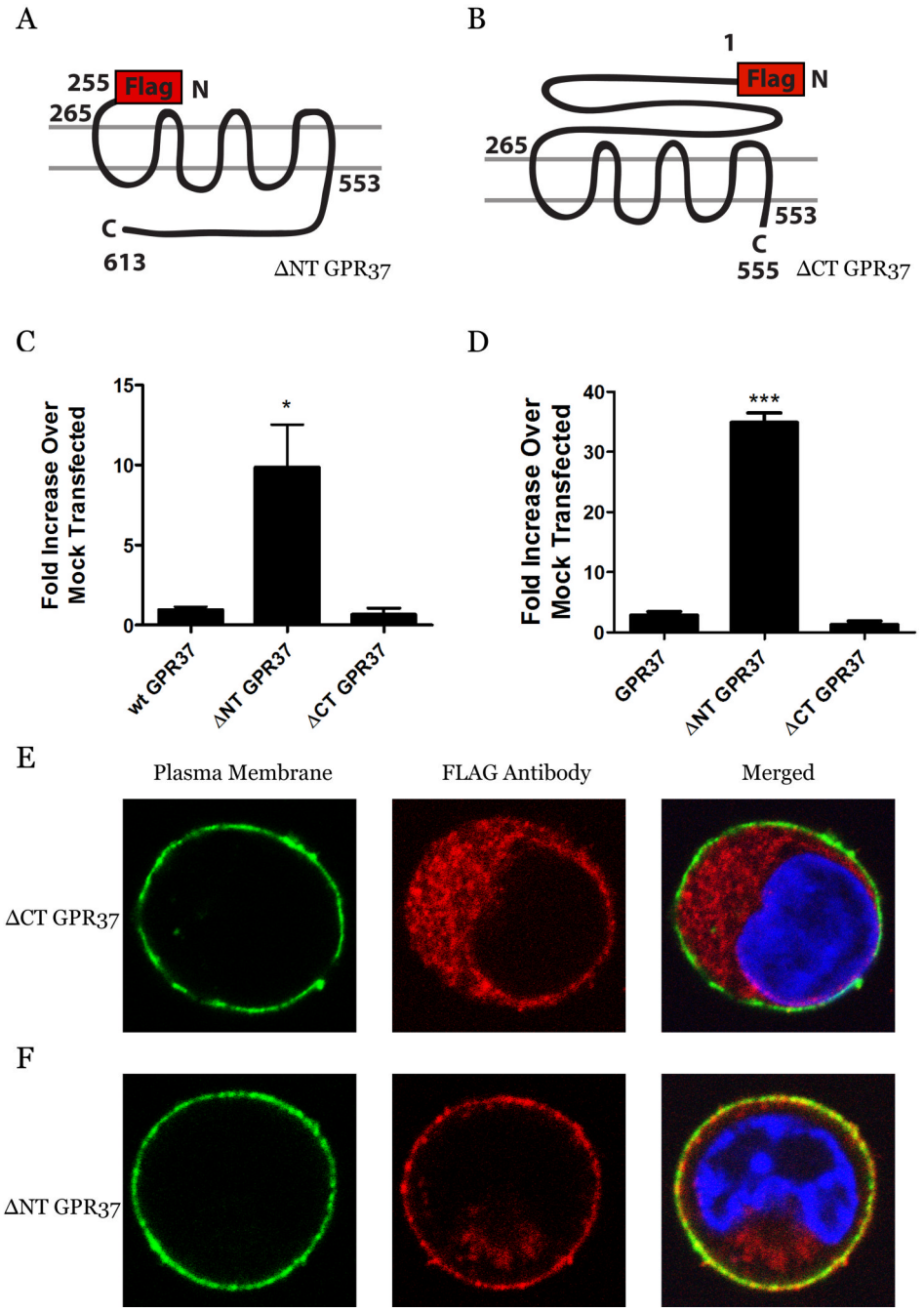

Fig. 2.

N-terminal truncation of GPR37 enhances plasma membrane expression. Constructs corresponding to N-terminal truncation *(A)* and C-terminal truncation (*B*) of GPR37 were prepared with N-terminal FLAG tags. HEK-293 cells were transiently transfected with wt GPR37, ΔNT GPR37, and ΔCT GPR37. Surface expression was detected using a luminometer-based assay (*C*) and via flow cytometry (*D*). Values are expressed as mean ± SEM for fold over wt GPR37. One-way ANOVA followed by Tukey's post-hoc test was used to determine statistical significance (n = 3–6; *, $p < 0.05$, ***, $p<0.0001$). Confocal imaging of cells transfected with ΔCT GPR37 (*E*) or ΔNT GPR37 (*F*) was done using mouse anti-Na^+/K^+ ATPase, followed by Alexa-Fluor 488, to mark the cell surface (green, left panels), rabbit anti-

FLAG, followed by Alexa-Fluor 546, to detect the receptors (red, center panels), and DAPI to stain the nucleus (blue, right panels). Yellow indicates colocalization of receptor with plasma membrane (E&F, right panels).

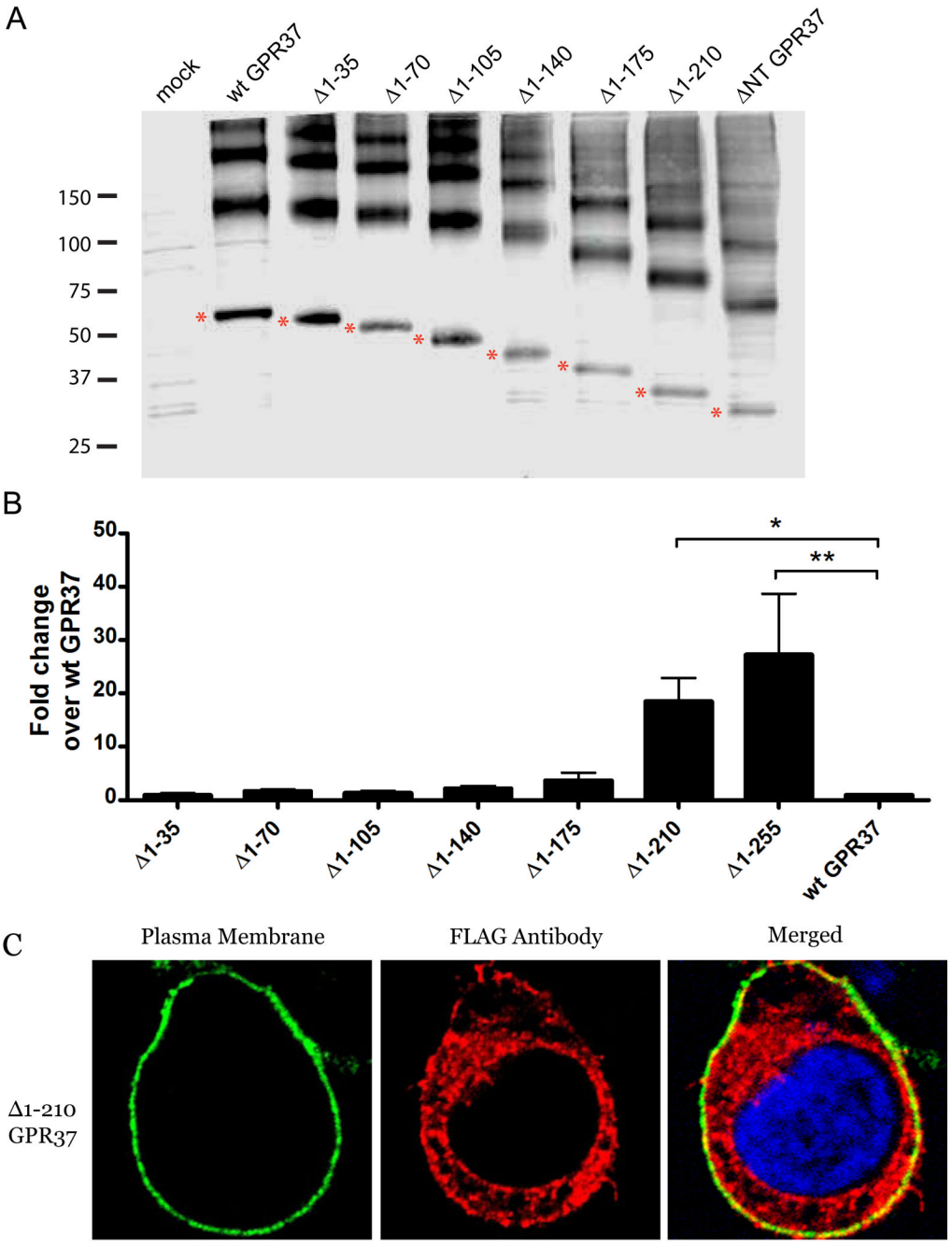

Fig. 3.

Regions on the GPR37 N-terminus influencing receptor surface expression. (*A*) Representative Western blot of N-terminal truncated constructs. HEK-293 cells expressing empty pCMV2b vector, wt GPR37, $\Delta^{1–35}$, $\Delta^{1–70}$, $\Delta^{1–105}$, $\Delta^{1–140}$, $\Delta^{1–175}$, $\Delta^{1–210}$, and ΔNT were harvested, run on SDS-PAGE gels, transferred, and blotted with anti-FLAG antibody. The monomeric species of interest is indicated with a red asterisk to the left of each band. Larger molecular weight species represent aggregated receptor, as is often seen for GPR37. (*B*) Surface expression of these receptors was determined using a luminometer-based assay. Values are expressed as mean ± SEM for fold increase over wt GPR37. One-way ANOVA followed by Dunnett's post-hoc test was used to determine statistical significance. ($n = 5$; *, $p < 0.05$; **, $p < 0.01$) Confocal

imaging of HEK-293 cells expressing $\Delta^{1–210}$ GPR37 (*C*) was done using mouse anti-Na^+/K^+ ATPase, followed by Alexa-Fluor 488, to mark the cell surface (green, left panel), rabbit anti-FLAG, followed by Alexa-Fluor 546, to detect the receptors (red, center panel), and DAPI to stain the nucleus (blue, right panel). Yellow indicates colocalization of receptor with plasma membrane (C, right panel).

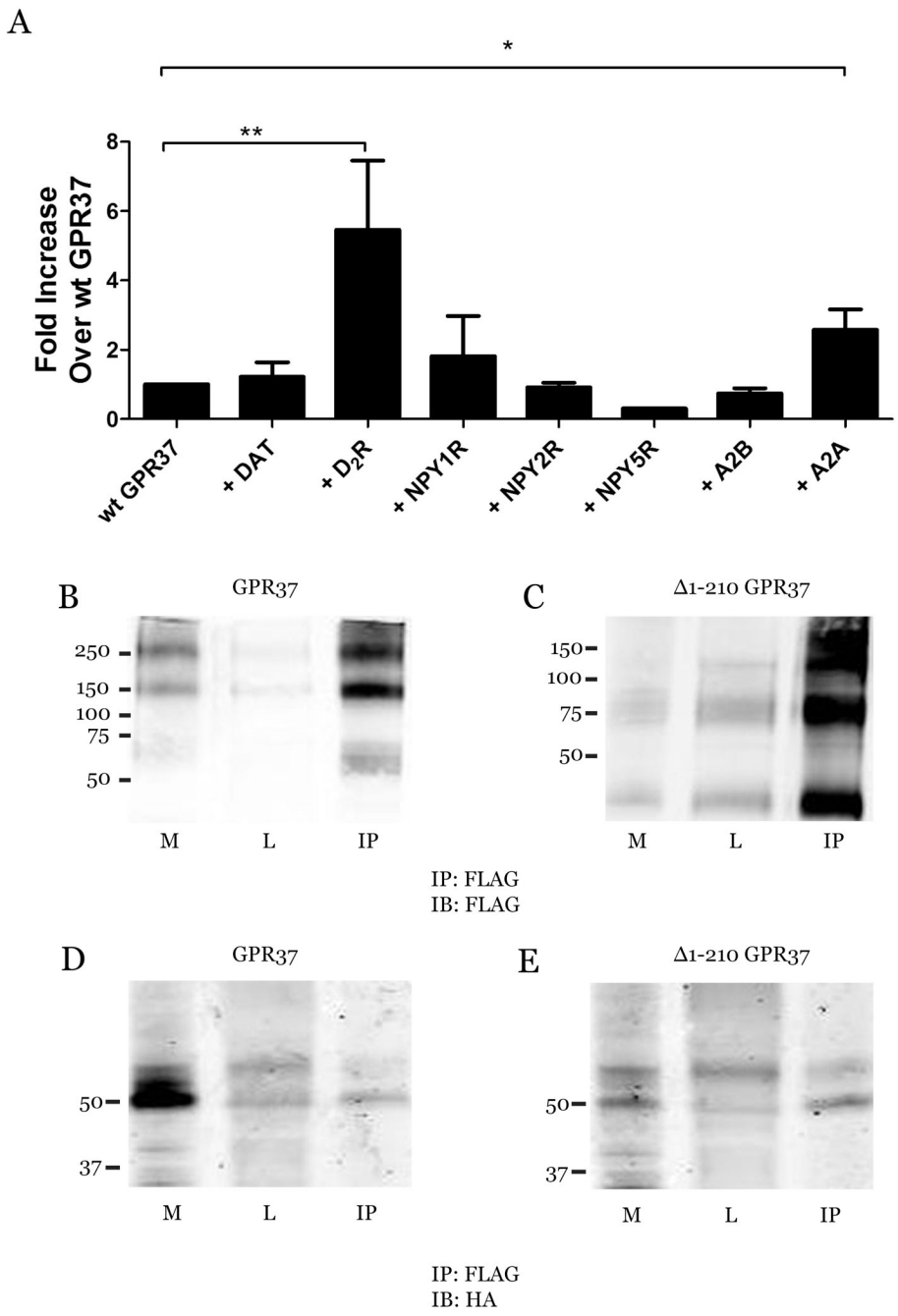

Fig. 4.

Physical association between D_2R and GPR37. HEK-293 cells were transiently transfected with FLAG-GPR37 ± DAT, HA-D_2R, HA-NPY_1, HA-NPY_2, HA-$A_{2B}R$ or HA-$A_{2A}R$. (*A*) Surface expression of GPR37 was determined using a luminometer-based assay. Values are expressed as mean ± SEM for fold increase over wt GPR37. A student's t-test was used to determine statistical significance (n = 3–8; *, $p < 0.05$; **, $p < 0.005$). (*B–E*) Cells were harvested, lysed, and immunoprecipitated (IP) with anti-FLAG antibody. Western blot detection of membrane (M), soluble lysate (L), and IP fractions with anti-FLAG (*B&C*) or anti-HA antibody (*D&E*) revealed robust co-immunoprecipitation of D_2R with both GPR37 (*B&D*) and mutant $\Delta^{1–210}$ GPR37 (*C&E*). The D_2R was observed at its expected molecular

weight of 48–52 kDa, with the different bands most likely corresponding to differentially-glycosylated forms of the receptor.

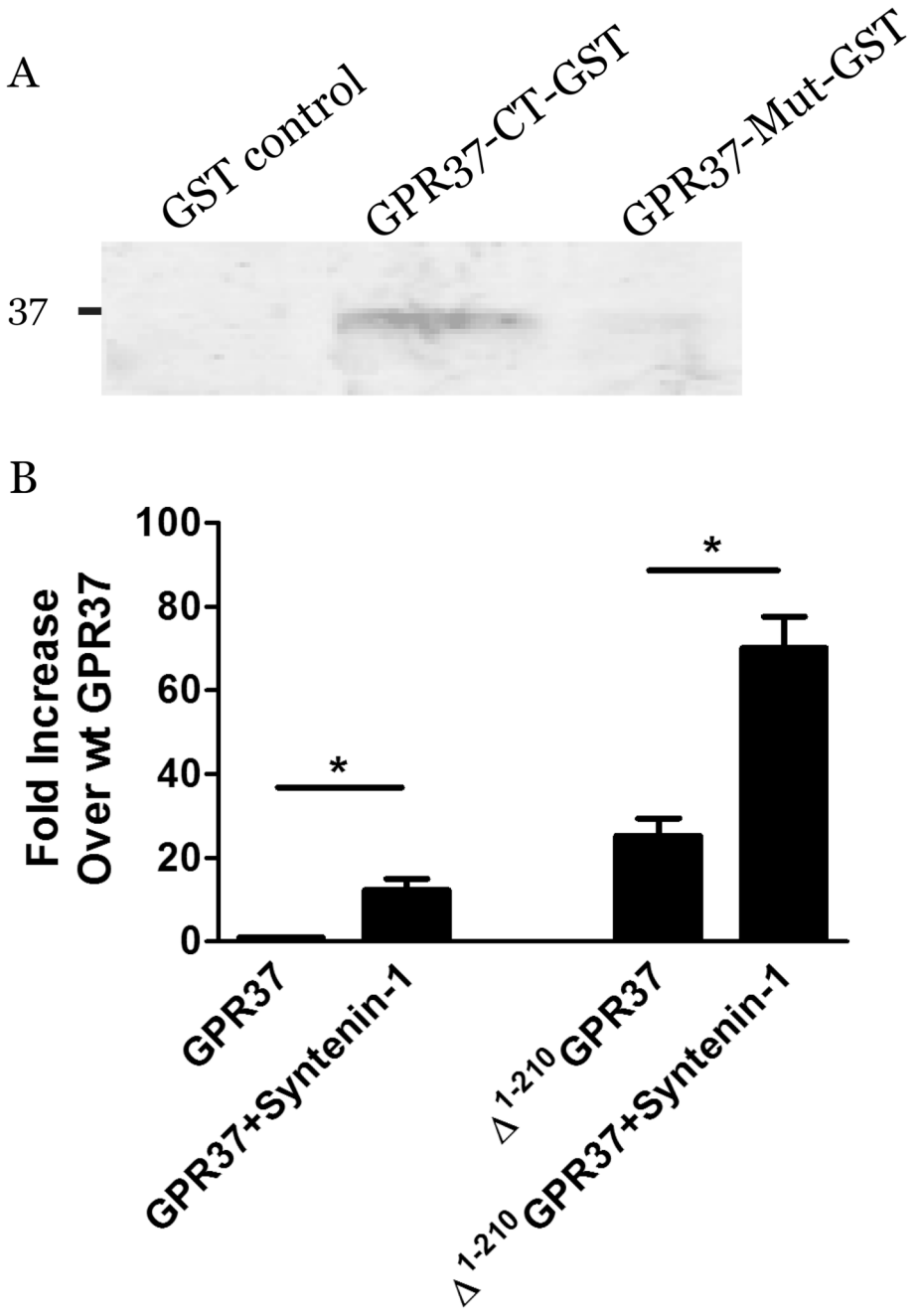

Fig. 5.

Physical association between GPR37 and syntenin-1. (*A*) Pull-down studies were performed examining syntenin-1 interactions with control GST, GPR37-CT-GST, and a mutant version of GPR37-CT-GST (GPR37-Mut-GST) with the PDZ-binding motif removed. Robust binding of syntenin-1 was observed only with wild-type GPR37-CT-GST. (*B*) HEK-293 cells were transiently transfected with wt GPR37 or Δ^{1-210} GPR37 in the absence and presence of co-expressed HA-syntenin-1. Surface expression of the receptors was determined using a luminometer-based assay. Values are expressed as mean ± SEM and as fold increase over wt GPR37 alone. (n = 3–4; *, $p < 0.05$).

Table 1

Co-expression with Δ^{1-210} GPR37 modulates D_2R ligand binding affinity.[a]

	D_2R	D_2R/GPR37	D_2R	D_2R/GPR37	D_2R	D_2R/GPR37
Agonists	Dopamine		Quinpirole			
K_i ± S.E.M. (nM)	97 ± 27	41 ± 10	82 ± 38	36 ± 9		
Antagonists	Haloperidol		Spiperone		YM-09151	
K_D/K_i ± S.E.M. (pM)	1114 ± 86	480 ± 76	72 ± 20	43 ± 10	1228 ± 567	621 ± 193

[a] Ligand-binding studies were performed, as described in *Materials and Methods*, on membranes derived from HEK-293 cells that had been transfected to transiently express HA-D_2R in the absence and presence of FLAG-Δ^{1-210} GPR37, due to the better expression of the truncated mutant of GPR37 and its robust association with D_2R. Estimates of K_i or K_D (± S.E.M.) for each ligand are provided. For the curves of dopamine and quinpirole displacement of ^{3}H-spiperone binding, two–site fits were not significantly better than one-site fits, therefore one-site fit values are shown.